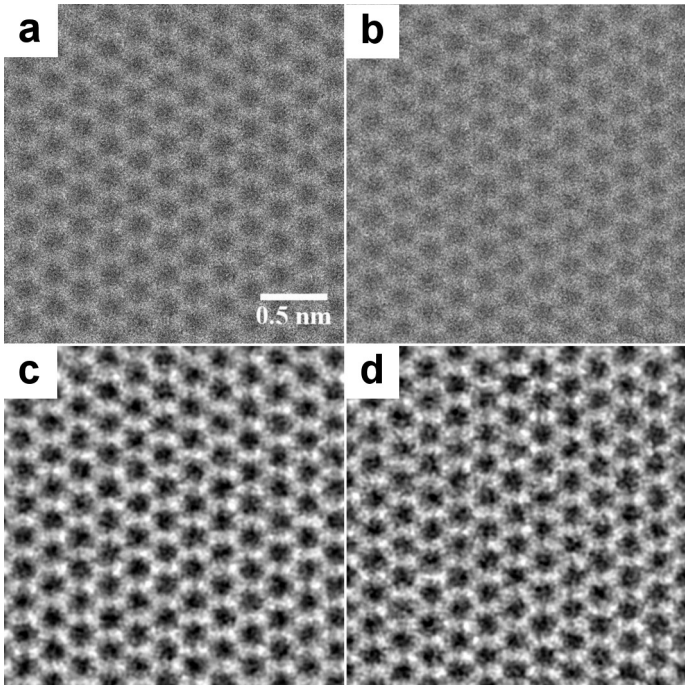

Supplementary figure S15: Scanning transmission electron microscope (STEM) single atom irradiation. STEM images of monolayer graphene (a) before and (b) after the STEM probe was focussed on to a single atom in a. (c,d) Processed images of a and b after a Fourier bandpass filter.

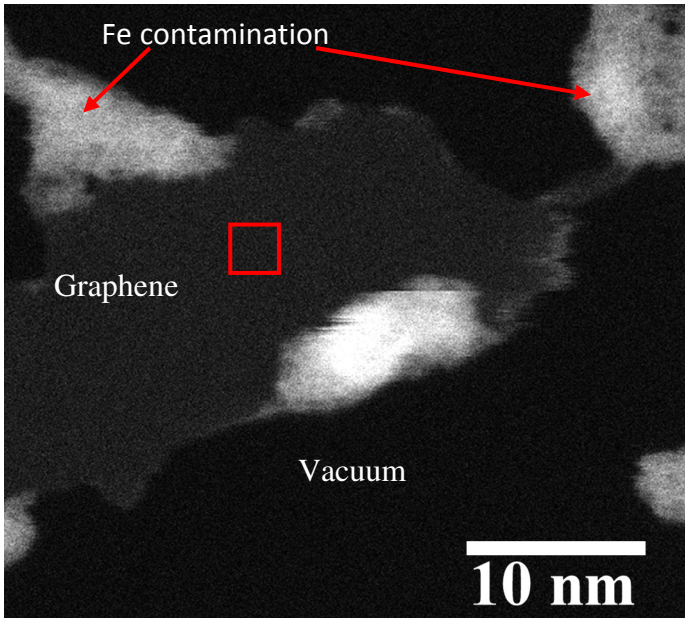

Supplementary figure S16: Chemically etched holes near the region of scanning transmission electron microscope (STEM) imaging. Angular dark field STEM image of graphene after 30 minutes of continual electron beam irradiation in the region shown by the red box. Holes (black) have opened up around the graphene (dark grey) that was imaged. Contamination, identified as Fe by electron energy loss spectroscopy (EELS), appears as lighter contrast.

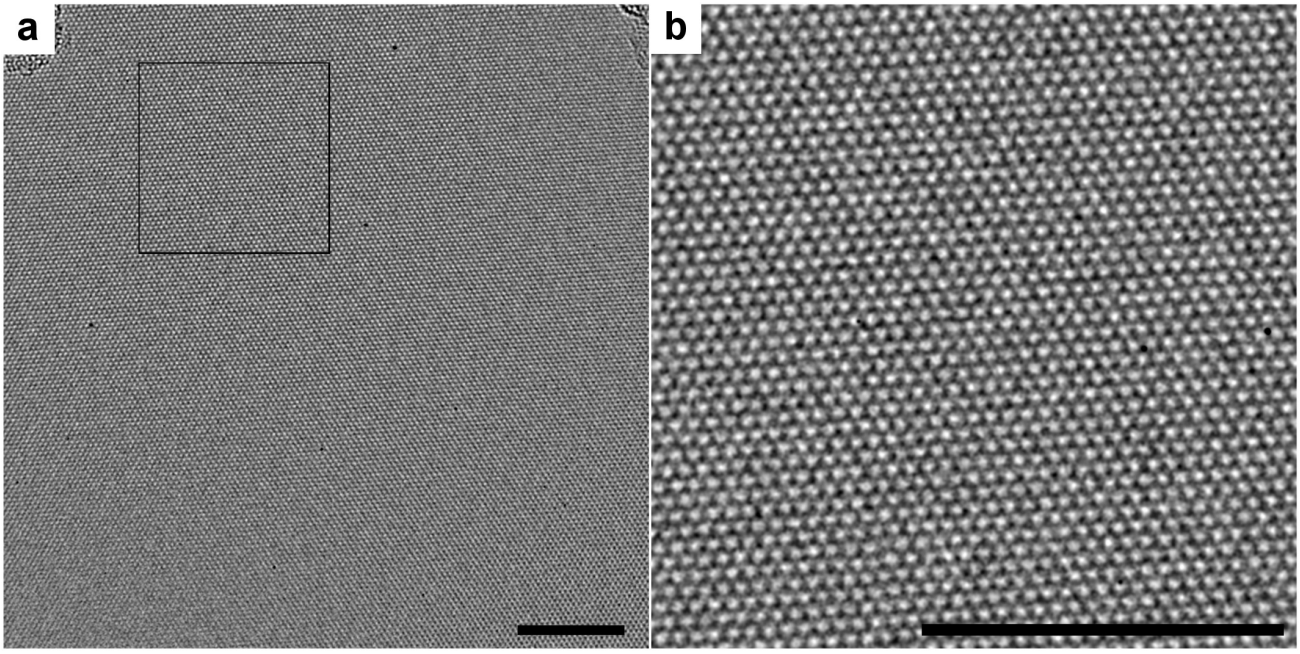

Supplementary figure S17: Low magnification aberration-corrected transmission electron microscope (AC-TEM) images of large area clean graphene. (a) An AC-TEM image of a large area of clean, uncontaminated graphene, demonstrating the effect of following the decontamination regime, with an area of ~ 10^3 nm^2 free of contamination. (b) The boxed region of (a) at a higher resolution. The bottom right of (a) has switched from white atom contrast to black. Scale bars denote 5 nm. The top right corner of (a) contains some residual contamination. More typically areas of at least 10^2 nm^2 are free from unwanted residue.

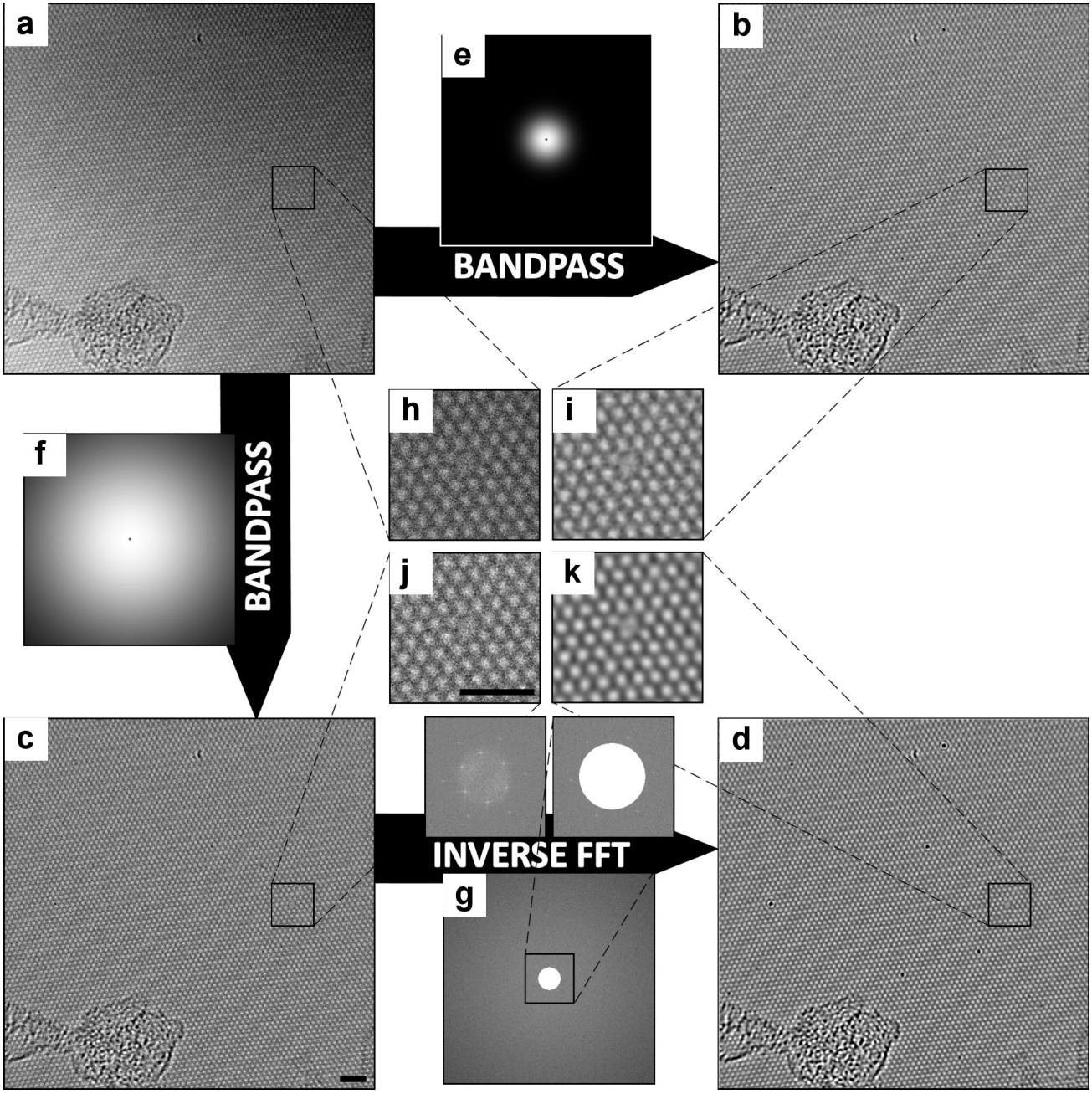

Supplementary figure S18: Aberration corrected transmission electron microscope (AC-TEM) image processing. A flow chart showing the two processing techniques used to analyse TEM images. (a) The as-recorded, unprocessed image. The path along the top demonstrates the application of a 100×5px bandpass filter, yielding (b), to remove both the brightness variation and high frequency noise. Alternatively, first a high pass filter is applied to remove brightness variation, giving (c), followed by the application of a positive mask to the {100} fringes to the fast Fourier transform (FFT), to yield a reconstructed image (d) that discards the more astigmatic higher resolution information. (e-g) Positive masks applied to the FFTs to filter the image. (h-k) Magnified views of the same divacancy structure for comparison. Scale bar denotes 1 nm.

Supplementary Discussion

Calculations of sputtering cross-section and beam induced heating

The sputtering cross section as a function of beam energy was calculated according to ref 31, taking into account out-of-plane atomic vibrations due to zero-point fluctuations in the Debye model approximation. Graphene flexural phonon modes exhibit a quadratic dispersion relationship and thus the Debye model will not exactly predict the correct mean-square-velocities. None-the-less it is still possible to gain valuable insights into the sputtering cross-section using the equations in ref 31. Supplementary figure S11 shows the cross-section as a function of beam energy for three different temperatures. In the Debye model, a temperature exceeding the Debye temperature of 1287 K is needed to thermally excite enough out-of-plane vibrations to generate the sputtering cross-section of 1.35×10^{-2} barn that we observe. Changing the threshold energy (supplementary figure S12) for sputtering affects the cross-section at a temperature of 300 K and incident electrons with 80 keV energy. A threshold energy of 19.7 eV leads to our observed cross-section of 1.35×10^{-2} barn.

Supplementary figure S13 shows how the sputtering-cross section depends upon the atomic mean-square-velocity, $\overline{v^2}$, for 80 keV incident electrons based on the Debye model. A $\overline{v^2}$ of ~2.7×10^{6} $m^2.s^{-2}$ is needed to produce the observed sputtering cross-section of 1.35×10^{-2} barn, which is approximately double that calculated at room temperature.

Supplementary figure S14 shows the negligible predicted temperature increase in our sample based on the model in ref 32. In our experiments the graphene is mounted on a silicon nitride (SiN) TEM grid rather than the more commonly used copper TEM grid. SiN has low thermal conductivity, and therefore the graphene is not in contact with a heat sink. This may impact on the results since the dissipation of heat may be restricted.

Supplementary Methods

Exposing single carbon atom to Angstrom focussed electron beam at 80 kV

In order to assess whether a monovacancy could be produced by only exposing a single carbon atom to an Angstrom sized electron probe, we used a JEOL JEM-ARM 200F TEM, equipped with both probe and image spherical aberration correctors operating at 80 kV in scanning transmission electron microscope (STEM) mode. We imaged monolayer graphene at high magnification, shown in supplementary figure S15a. The location of a single carbon atom was identified from the image and then the STEM probe was positioned such as to expose only a single atom for 5 minutes. A probe current of 32 pA was used. After exposure the area was imaged again, shown in supplementary figure S15b. Supplementary figures S15c,d show supplementary figures S15a,b after applying a Fourier bandpass filter. We then repeated this 3 times and in all cases no defects were observed in the area exposed. A 32 pA probe current with an Angstrom diameter probe gives a beam current density of ~ 2.54×10^{10} e^{-} nm^{-2} s^{-1}, which is two orders of magnitude more than achieved using the focused TEM probe. This indicates that it is not just the beam current density received by a single atom that is important, but also the area of the sample that is exposed to a high beam current density. However, holes were found in the surrounding area of the graphene, where Fe contamination was present, shown in supplementary figure S16. The area where the holes formed was not exposed to any substantial electron beam irradiation. The red box in supplementary figure S16 shows where the electron beam was confined to for 30 minutes. This indicates that the chemical etching process that is known to form the holes in graphene does not require direct exposure of the electron beam.

Notes on graphene decontamination

Annealing the sample is an effective method for removing PMMA residue; however, residual iron from the $FeCl_3$ etch phase caught on the graphene film act as etching centres at high temperatures, causing the formation of the holes.[42,43] Removal of the iron is done by applying a HCl rinsing stage after transfer from the $FeCl_3$ solution, allowing for long bake periods without the formation of holes. Supplementary figure S17 demonstrates the effect of employing this graphene decontamination

regimen, showing an area of ~ 10^3 nm^2 free of contamination. This helped to reduce the frequency of chemically etched holes during exposures to the electron beam.

Image Processing

The AC-TEM images presented have been subjected to the image filtering procedure outlined in supplementary figure S18. The procedure resulting in figure S18d was used in processing the images displayed in the figures of this work. The bandpass filter was used for additional verification that processing was not causing image processing artefacts to be misinterpreted as defects.